Structural Flexibility of the Pentameric SARS Coronavirus Envelope Protein Ion Channel

Krupakar Parthasarathy,* Lifang Ng,* Xin Lin,* Ding Xiang Liu,[†] Konstantin Pervushin,* Xiandi Gong,* and Jaume Torres*

*School of Biological Sciences, Nanyang Technological University, Singapore; and [†]Institute of Molecular Cell Biology, Proteos, Singapore

ABSTRACT   Coronaviruses contain a small envelope membrane protein with cation-selective ion channel activity mediated by its transmembrane domain (ETM). In a computational study, we proposed that ion channel activity can be explained by either of two similar ETM homopentameric transmembrane α-helical bundles, related by a ~50° rotation of the helices. Later, we tested this prediction, using site-specific infrared dichroism of a lysine-flanked isotopically labeled ETM peptide from the virus responsible for the severe acute respiratory syndrome, SARS, reconstituted in lipid bilayers. However, the data were consistent with the presence of a kink at the center of the ETM α-helix, and it did not fit completely either computational model. Herein, we have used native ETM, without flanking lysines, and show that the helix orientation is now consistent with one of the predicted models. ETM only produced one oligomeric form, pentamers, in the lipid-mimic detergent dodecylphosphocholine and in perfluorooctanoic acid. We thus report the correct backbone model for the pentameric α-helical bundle of ETM. The disruptive effects caused by terminal lysines probably highlight the conformational flexibility required during ion channel function.

Coronaviruses are enveloped viruses responsible for a variety of acute and chronic diseases (1). Their members have an envelope (E) protein, embedded in the membrane, which is critical for virion morphogenesis (2,3). These E proteins have also shown cation-selective ion channel activity, not only in the virus causative of severe acute respiratory syndrome (SARS), but also in other members of the coronavirus genus (4,5). Ion channel activity is inhibited by the drug hexamethylene amiloride (HMA) in murine hepatitis virus and in human coronavirus 229E, and this inhibition was correlated with decreased viral replication in these viruses. Also, HMA did not have antiviral activity against a recombinant murine hepatitis virus where E protein had been deleted (5), pointing to coronavirus E proteins as a pharmacological target.

In severe acute respiratory syndrome (SARS), the E protein has 76 amino acids, and contains one transmembrane α-helical domain (ETM), which is responsible for the observed ion channel activity (4,6) via the likely formation of a transmembrane α-helical bundle. In a recent computational work (7), we suggested possible models for ETM oligomerization by exploring exhaustively the conformational space of several ETM oligomers (8). This search was run in parallel with homologous sequences of ETM present in other coronaviruses, on the assumption that they share a common backbone structure (9). Conservative mutations that appear during evolution act as a filter, destabilizing nonnative models. At the same time, these mutations leave unaffected those models representing the native backbone structure. Under these evolutionary constraints, only two models compatible with ion channel activity were found, both pentameric, referred to as models A and B (7). These two models had the same handedness and similar helix tilt, and were related by a ~50° rotation of their α-helices (7) (see Table 1, Models A and B). In 14 out of 15 ETM homologous sequences, lowest-energy models clustered around model A (11), which was therefore likely to represent the native backbone structure of the ETM ion channel.

To test our computational prediction, we performed recently a site-specific infrared dichroism study (12) of ETM in the SARS E sequence, reconstituted in dimyristoylphosphatidylcholine lipid bilayers. ETM was isotopically-labeled with $^{13}C=^{18}O$ (10), at nine native residues, except at F-23, where we used Ala because of the lack of labeled Phe. In addition, to facilitate purification (13), ETM was flanked by two lysines at each N- and C termini (K_2-ETM-K_2), as it has been shown for various α-TM oligomers that even four flanking lysines at each C- and N-terminus do not affect oligomerization during SDS-PAGE (14,15). Although the rotational orientation (12), ω, of the centrally located labels was consistent with one of the models (B), labels located at the N- and C-ends of the TM were consistent with model A (10), suggesting a mild twist, or kink, in a region of the helix near residue F-23 (see Table 1, column K_2-ETM-K_2 (A-23)).

To test the possible effect of the mutation F-23A on ETM structure, we have studied herein the same peptide, K_2-ETM-

K_2, but using the native F-23 residue isotopically labeled with $^{13}C=^{18}O$. We note that the use of label F-23, instead of A-23, should not only affect the ω value at F-23, but also the calculated value for the preceding and following residue. Indeed, the rotational orientation, ω, is calculated by combining two consecutive residues (12), which are assumed to be separated by $\Delta\omega = 100°$ for canonical α-helices. The infrared spectra obtained for K_2-ETM-K_2 were similar to those obtained previously (10), and are not shown.

Thus, from the measured dichroic ratios of the K_2-ETM-K_2 sample, R_{helix} and R_{site} (shown in the Supplementary Material, Table 1, Data S1), we recalculated the orientational data for the labeled residues 22 and 24 (10). Table 1 (column K_2-ETM-K_2 (F-23)) shows that the recalculated ω values are still incompatible with either model A or B.

Next, to test the effect of terminal lysine residues on ETM structure, we used the SARS ETM peptides shown in Fig. 1, where terminal lysines have been substituted to native ETM residues. These peptides were labeled independently at five native consecutive residues: L-21, A-22, F-23, V-24, and V-25.

The data were analyzed as above (dichroisms are shown in the Supplementary Material, Table 1, Data S1), and the calculated ω values are indicated in the last column of Table 1 (ETM). These values are clearly consistent with model A; therefore, we conclude that the presence of terminal lysines in K_2-ETM-K_2 introduces a perturbation in the ETM structure, at least from residues 19 to 24. Consistent with this, solution NMR results of ETM in dodecylphosphocholine (DPC) micelles also indicate a kink in the central part of the α-helix in the peptide K_2-ETM-K_2, but not in ETM (Fig. S1, Data S1).

To confirm that ETM forms pentamers, we performed a sedimentation equilibrium study in DPC micelles. DPC is a mimic for dimyristoylphosphatidylcholine, as it has the same polar headgroups, and has been routinely used to determine oligomeric size of TM α-helices, e.g., (16). The sedimen-
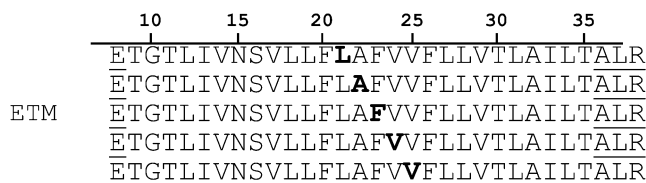
TABLE 1

Residue	Model A	Model B	K_2-ETM-K_2 (A-23)	K_2-ETM-K_2 (F-23)	ETM
V-17	−31	−80	−47 ± 5		
L-18	57	8	15 ± 8		
L-19	164	110	105 ± 3		
F-20	−78	−132			
L-21	6	−30	−44 ± 4		4 ± 4
A-22	106	60	50 ± 7	−22 ± 7	113 ± 8
F-23	−128	−183	−170 ± 7	−76 ± 7	−109 ± 7
V-24	−32	−83	−70 ± 4	24 ± 4	−6 ± 5
V-25	80	22			94 ± 5
F-26	−173	130			
L-27	−64	−113	−48 ± 4		
L-28	22	−15	52		

Rotational orientation values, ω, for the predicted pentameric models A and B (7), experimental values from K_2-ETM-K_2 using label A-23 (10), from K_2-ETM-K_2 using native label F23 (this work), and native ETM without flanking lysines (this work). The helix tilt for the last two columns was 20–25° and is not shown.
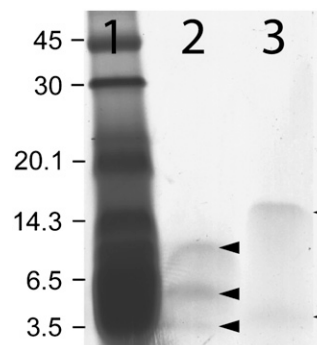
```
              10      15      20      25      30      35
      ETGTLIVNSVLLFLAFVVFLLVTLAILTALR
      ETGTLIVNSVLLFLAFVVFLLVTLAILTALR
ETM   ETGTLIVNSVLLFLAFVVFLLVTLAILTALR
      ETGTLIVNSVLLFLAFVVFLLVTLAILTALR
      ETGTLIVNSVLLFLAFVVFLLVTLAILTALR
```

FIGURE 1 Synthetic peptide sequences of SARS ETM, with isotopically ($^{13}C=^{18}O$) labeled residues indicated in bold, used for site-specific infrared dichroism. N- and C-terminal lysines used in a previous work (10) have been changed to the residues underlined, which correspond to native SARS ETM residues.

tation data could be best fitted to a monomer-pentamer self-association model, with an association constant of 17.1 (Fig. S2, Data S1), although a higher order aggregate ($n > 10$) was also present (~10% of the material) at high concentrations of the peptide (not shown).

We also performed electrophoresis of ETM in the mild detergent perfluorooctanoic acid (PFO). Although less suitable than zwitterionic DPC, this detergent has been successfully used to determine the oligomeric sizes of α-helical transmembrane peptides, e.g., in the tetrameric phospholemman (17), or the pentameric small hydrophobic protein in the respiratory syncytial virus (18), which in SDS produced either monomers or multiple nonspecific oligomers, respectively. Fig. 2 shows that the only oligomer of ETM in PFO is pentameric (*lane 3*). By contrast, in K_2-ETM-K_2 (*lane 2*), the pentamer was not stable, and only produced dimers and trimers. Results in SDS were identical as those described previously (6,7,10) and are shown in Fig. S4 (Data S1).

These results suggest that the terminal lysines in K_2-ETM-K_2 not only induce a kink in the ETM α-helix, but also may weaken interhelical interactions. These two effects, however, do not inactivate the ETM ion channel present in lipid bilayers, because K_2-ETM-K_2 shows sodium ((6) and Fig. S5, Data S1) conductance activity, which was blocked by amantadine (6). ETM, however, displayed a different

FIGURE 2 Electrophoresis of ETM in PFO. Lane 1, molecular weight markers; lane 2, K_2-ETM-K_2; and lane 3, ETM without lysines(see Fig. 1). Arrows indicate monomers, dimers, and trimers (*lane 2*), and monomers and pentamers (*lane 3*).

conductance behavior relative to K_2-ETM-K_2, with an open probability that was proportional to the potential (Fig. S5, panel *d*, Data S1). By contrast, in K_2-ETM-K_2, this dependency was lost. In addition, amantadine was less effective as an inhibitor for ETM than for K_2-ETM-K_2 (Fig. S6, Data S1).

Overall, our results show that flanking lysines induce a kink in ETM and weaken interhelical interactions. The precise origin of these effects is unknown, but it is likely related to the interaction of lysine side chains with the phosphocholine interface headgroups. These effects may unveil the presence of inherent conformational plasticity in ETM, possibly required during ion channel function, as suggested for other ion channels (19,20). Indeed, the central region of ETM, i.e., two turns from residue 19 to 26, contains three phenylalanines (bulky) and two valines (β-branched), which are known to destabilize α-helices (21).

Our previous results (6) indicate that amantadine has more affinity for this lysine-induced conformational state than for the model represented by the native ETM, model A (10). This could explain the observed lack of protection of amantadine against SARS-induced cytopathic effects (22). A more detailed NMR study of the structure of this channel, complexed with the inhibitory drug HMA, is under way.

SUPPLEMENTARY MATERIAL

To view all of the supplemental files associated with this article, visit www.biophysj.org.

ACKNOWLEDGMENTS

REFERENCES and FOOTNOTES

1. Siddell, S. G. 1995. The Coronaviridae; An Introduction. Plenum Press, New York.

2. Lim, K. P., and D. X. Liu. 2001. The missing link in coronavirus assembly. Retention of the avian coronavirus infectious bronchitis virus envelope protein in the pre-Golgi compartments and physical interaction between the envelope and membrane proteins. *J. Biol. Chem.* 276:17515–17523.

3. Corse, E., and C. E. Machamer. 2001. Infectious bronchitis virus envelope protein targeting: implications for virus assembly. *Adv. Exp. Med. Biol.* 494:571–576.

4. Wilson, L., C. McKinlay, P. Gage, and G. Ewart. 2004. SARS coronavirus E protein forms cation-selective ion channels. *Virology.* 330:322–331.

5. Wilson, L., P. Gage, and G. Ewart. 2006. Hexamethylene amiloride blocks E protein ion channels and inhibits coronavirus replication. *Virology.* 353:294–306.

6. Torres, J., U. Maheswari, K. Parthasarathy, L. Ng, D. X. Liu, and X. Gong. 2007. Conductance and amantadine binding of a pore formed by a lysine-flanked transmembrane domain of SARS coronavirus envelope protein. *Protein Sci.* 16:2065–2071.

7. Torres, J., J. Wang, K. Parthasarathy, and D. X. Liu. 2005. The transmembrane oligomers of coronavirus protein E. *Biophys. J.* 88:1283–1290.

8. Adams, P. D., I. T. Arkin, D. M. Engelman, and A. T. Brunger. 1995. Computational searching and mutagenesis suggest a structure for the pentameric transmembrane domain of phospholamban. *Nat. Struct. Biol.* 2:154–162.

9. Briggs, J. A. G., J. Torres, and I. T. Arkin. 2001. A new method to model membrane protein structure based on silent amino acid substitutions. *Proteins Struct. Funct. Genet.* 44:370–375.

10. Torres, J., K. Parthasarathy, X. Lin, R. Saravanan, A. Kukol, and D. X. Liu. 2006. Model of a putative pore: the pentameric α-helical bundle of SARS coronavirus E protein in lipid bilayers. *Biophys. J.* 91:938–947.

11. Torres, J., J. A. G. Briggs, and I. T. Arkin. 2002. Contribution of energy values to the analysis of global searching molecular dynamics simulations of transmembrane helical bundles. *Biophys. J.* 82:3063–3071.

12. Arkin, I. T., K. R. MacKenzie, and A. T. Brunger. 1997. Site-directed dichroism as a method for obtaining rotational and orientational constraints for oriented polymers. *J. Am. Chem. Soc.* 119:8973–8980.

13. Therien, A. G., and C. M. Deber. 2002. Oligomerization of a peptide derived from the transmembrane region of the sodium pump gamma subunit: effect of the pathological mutation G41R. *J. Mol. Biol.* 322:583–590.

14. Melnyk, R. A., A. W. Partridge, and C. M. Deber. 2001. Retention of native-like oligomerization states in transmembrane segment peptides: application to the *Escherichia coli* aspartate receptor. *Biochemistry.* 40:11106–11113.

15. Melnyk, R. A., A. W. Partridge, J. Yip, Y. Wu, N. K. Goto, and C. M. Deber. 2003. Polar residue tagging of transmembrane peptides. *Biopolymers.* 71:675–685.

16. Kochendoerfer, G. G., D. Salom, J. D. Lear, R. Wilk-Orescan, S. B. Kent, and W. F. DeGrado. 1999. Total chemical synthesis of the integral membrane protein influenza A virus M2: role of its C-terminal domain in tetramer assembly 1. *Biochemistry.* 38:11905–11913.

17. Beevers, A. J., and A. Kukol. 2006. Secondary structure, orientation, and oligomerization of phospholemman, a cardiac transmembrane protein. *Protein Sci.* 15:1127–1132.

18. Gan, S. W., L. Ng, L. Xin, X. Gong, and J. Torres. 2008. Structure and ion channel activity of the human respiratory syncytial virus (hRSV) small hydrophobic protein transmembrane domain. *Protein Sci.* 17:813–820.

19. Li, C., H. Qin, F. P. Gao, and T. A. Cross. 2007. Solid-state NMR characterization of conformational plasticity within the transmembrane domain of the influenza A M2 proton channel. *Biochim. Biophys. Acta.* 1768:3162–3170.

20. Cady, S. D., and M. Hong. 2008. Amantadine-induced conformational and dynamical changes of the influenza M2 transmembrane proton channel. *Proc. Natl. Acad. Sci. USA.* 105:1483–1488.

21. Chellgren, B. W., and T. P. Creamer. 2006. Side-chain entropy effects on protein secondary structure formation. *Proteins.* 62:411–420.

22. Tan, E. L., E. E. Ooi, C. Y. Lin, H. C. Tan, A. E. Ling, B. Lim, and L. W. Stanton. 2004. Inhibition of SARS coronavirus infection in vitro with clinically approved antiviral drugs. *Emerg. Infect. Dis.* 10:581–586.